8th International Symposium on Magnetic Bearing
August 26-28, 2002, Mito, Japan

DESIGN OF AN AXIAL-TYPE SELF-BEARING MOTOR FOR SMALL AXIAL PUMP

Kunihiro Ohmori
Dept. of Mechanical Eng., Ibaraki University, Hitachi, Ibaraki-Pref., 316-8511 Japan
koomori@mech.ibaraki.ac.jp

Seung-Jong Kim
Tribology Research Center, Korean Institute of Science and Technology, Seoul, 136-791 Korea
sjongkim@kist.re.kr

Toru Masuzawa
Dept. of Mechanical Eng., Ibaraki University, Hitachi, Ibaraki-Pref., 316-8511 Japan
masuzawa@mech.ibaraki.ac.jp

Yohji Okada
Dept. of Mechanical Eng., Ibaraki University, Hitachi, Ibaraki-Pref., 316-8511 Japan
okada@mech.ibaraki.ac.jp

ABSTRACT

Aiming at a small axial pump with a levitated rotor which is leading to a small artificial heart, this paper introduces a design scheme for an axial-type self-bearing motor. The axial type, which is basically composed of a disc motor and an axial magnetic bearing, controls both the rotation and the axial translation of a rotor. Considering that main requirements for the targeted axial pump are small size under 30 mm in diameter and high rotational speed over 10,000 rpm, we designed the system with a bidirectional structure, which consisted of two opposite stators and a rotor between them. Finally, the experimental setup is made to confirm the capability of the proposed motor. The experimental results show that the bidirectional axial-type self-bearing motor has high capability for a small axial blood pump.

INTRODUCTION

Several types of the artificial heart have been developed for long term ventricular assist systems. For the application to the artificial heart pump, major requirements are high durability, high reliability of the mechanics and compact size for implant. Because the blood pump should be implanted inside the patient's body for long term without any maintenance. A continuous flow type pump is able to reduce size of the device because pump volume is unnecessary. However, in order to support a rotating shaft, the continuous flow type pump requires mechanical bearings and the mechanical bearings cause serious problems about durability. Therefore, several groups in the world are trying to develop a magnetically suspended continuous flow type blood pumps with a self-bearing motor. The self-bearing motors are divided into radial and axial types by an actively controlled direction. The radial self-bearing motors actively control two degree-of-freedom motions of a rotor in radial directions. While, the other directional motions are supported by another passive or active magnetic bearings. In general, this radial type motor produces not only the motor torque but also the stabilizing force from rotating magnetic fluxes. Thus, it requires a complex construction of a stator and control mechanism. It means that the radial type self-bearing motor has the drawback in miniaturizing the system and increasing reliability. On the other hand, the axial type self-bearing motor, which is basically composed of a disc motor and an axial magnetic bearing, controls both the rotation and the axial translation of a rotor. To stabilize the rotor completely, additive magnetic bearings are also needed just like in the radial type. Such an axial type self-bearing motor has a simpler control mechanism as well as a smaller structure, than the radial type, since it treats only a single rotating magnetic flux.

Aiming at application to a small axial pump, this paper introduces a design scheme of the axial type self-bearing motor. Since the main requirements for

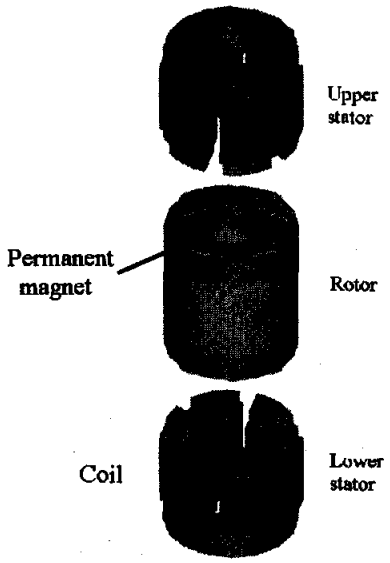

FIGURE 1: Schematic diagram of a bidirectional axial-type self-bearing motor

the pump are small size under 30 mm in diameter and high rotational speed over 10,000 rpm, the motor is designed to be a bidirectional type, which consists of two opposite stators and a rotor between them. In this type, the resultant axial magnetic force is the difference between the two attractive axial forces, while the motor torque is doubled in magnitude. Thus, it is suitable for a system demanding both simple structure and relatively high torque.

AXIAL TYPE SELF-BEARING MOTOR

Figure 1 shows the schematic structure of rotor and stator of the bidirectional axial type self-bearing motor. This motor consists of two opposite stators and a rotor between them. On both upper and lower surfaces, the rotor has four permanent magnets which are two N poles and two S poles by turns. The shape of permanent magnets was designed so that they could give nearly sinusoidal flux distribution. On the other hand, each stator has six cores with three phase windings to generate a four pole rotating magnetic flux in the air gap. The fluxes from the stator windings and the permanent magnets produce the motoring torque to the rotor and generates the attractive force between the rotor and the stator. Rotation principle is exactly the same as the theory of a general four pole three phase synchronus motor. Levitation principle is the same as the theory of an axial type active magnetic bearing. Therefore, a position feedback control is necessary to stabilize the axial motion of the rotor. In bidirectional type, the resultant axial magnetic force is the difference between the two attractive forces, while motoring torque is double in magnitude.

The tilting and the radial motion of the rotor is passive controlled. Note that the rotor must be sufficiently long to ensure passive stability in tilting motion. However, for small size, shorter length is preferable.

Since a single rotating magnetic flux is capable of generating both the motoring torque and axial force, axial-type self-bearing motor has simpler construction and control system.

Axial force and motoring torque

Assuming that the magnetic flux density B_r generated by permanent magnets of the rotor is sinusoidal, it is written as

$$B_r(\theta, t) = B_R cos(\omega t - 2\theta) \quad (1)$$

where B_R is the peak value of B_r, ω is a rotating speed in rad/s, and θ is an angular position from the center of the core with U phase in the stationary coordinate. Similarly, the magnetic flux density B_s generated by the stator windings is written as

$$B_s(\theta, t) = B_S cos(\omega t - 2\theta - \psi) \quad (2)$$

where B_S is the peak value of B_s and ψ is the phase difference between B_r and B_s.

Then, considering the magnetic energy stored in the uniform air gap in the single stator case leads to the simple expressions of the axial force F and the motoring torque T as

$$F = \frac{A_r}{4\mu_0}(B_R^2 + 2B_R B_S cos\psi + B_S^2) \quad (3)$$

$$T = \frac{A_r g_0}{2\mu_0} B_R B_S sin\psi \quad (4)$$

where A_r is an area of the rotor, μ_0 is the permeability of free space, and g_0 is an air gap between stator and rotor. The above relations denote that both axial force and motoring torque are controlled by changing the amplitude and the phase of the currents in the stator, even if not separately.

Now, let us extend the axial force of Eq. (3) and the motoring torque of Eq. (4) to the bidirectional case. The peak value B_S of Eq. (2) can be written about the upper and lower stators as

$$B_{S_{upper}} = B_M + B_C \quad (5)$$

$$B_{S_{lower}} = B_M - B_C \quad (6)$$

where $B_{S_{upper}}$ and $B_{S_{lower}}$ mean the magnetic flux densities of the upper and lower stators, respectively, B_M is a normal value of magnetic flux producing

TABLE 1: Design parameters

parameter	value
outer diameter	$28[mm]$
inner diameter	$14[mm]$
rotor area	$462[mm^2]$
core area	$49[mm^2]$
No. of coil turns	50
thickness of P.M.	$0.7[mm]$
P.M. area	$70[mm^2]$
specific permeability of P.M.	1.05

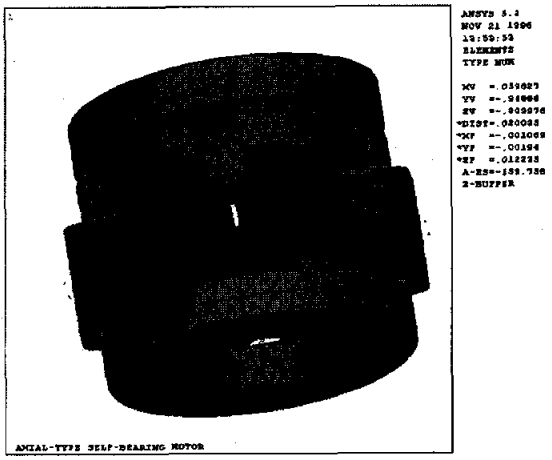

FIGURE 2: Solid elements created for the numerical analysis

motoring torque, and B_C is a magnetic flux density for levitation control. Suppose that all conditions are the same in both stators, from the equations (3) and (4), we have,

$$F_{total} = \frac{A_r}{\mu_0}(B_R cos\psi + B_M)B_C \quad (7)$$

$$T_{total} = \frac{A_r}{\mu_0}B_R B_M sin\psi \quad (8)$$

where F_{total} and T_{total} are the total torque and force. Note that in this case, one can control the axial motion of the rotor, not affecting the motoring torque. Although these expressions may have some inaccuracy on account of heavy assumptions, they provide a good guideline on the design of control system.

Analysis of Magnetic Field

As mentioned before, main requirements for design of the axial-type self-bearing motor are the small diameter and the enough torque. In general, a small-sized system often causes large modeling error by

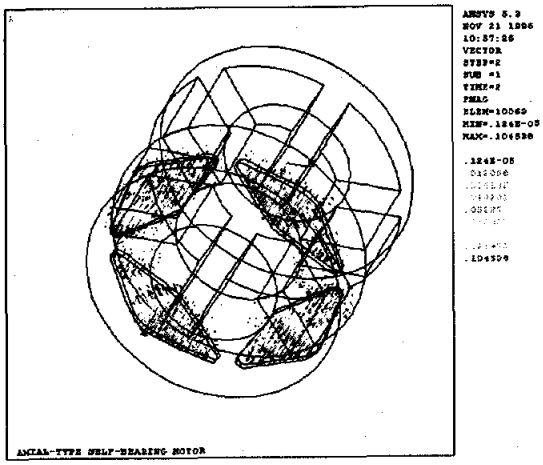

FIGURE 3: Estimated magnetic force and torque when $\psi = 90[deg]$

leakage and nonlinear effect that could not be neglected so far. In addition, since the motor torque is in proportion to the cube of radius of a rotor, it is necessary to carefully estimate the performance prior to manufacture, in particular, for such a small and high speed motor. For this purpose, we carried out finite element analysis of magnetic fields with the aid of ANSYS package.

The space to be analyzed involves not only the solid objects, i.e. a rotor and a stator including four permanent magnets and six current sources, respectively, but also the air part surrounding them. Figure 2 shows the created elements of the solid parts. Table 1 lists the design parameters used for the analysis. Figure 3 shows the finally adopted result depicting the distribution of magnetic force acting on the surfaces of the stator, where each arrow means a force vector at that point. Table 2 lists the Maxwell force components calculated by using an ANSYS, and the torque obtained from the force data subsequently. Note that the results in Table 2 are in the case of y = 90 ° which gives the maximum torque. As a result, the analyzed self-bearing motor was estimated to have the attractive force of 13.0 N at least and the torque of 8.69 Nmm maximum at normal state. Here, remember that in the bidirectional type, the maximum torque will be doubled.

EXPERIMENTAL SETUP AND RESULTS

Figure 4 shows schematic diagram of an experimental setup, which is the bidirectional type. This system consists of two opposite stator and a rotor between them. On both upper and lower surfaces, the rotor has four permanent magnets. And it has four eddy current type displacement sensors, which are

TABLE 2: Estimated magnetic force and torque when $\psi = 90[deg]$

core number	maxwell force $[N]$			torque $[Nmm]$
	radial-x	radial-y	axial-z	
1	−0.190	−0.227	1.23	2.70
2	0.158	−0.258	2.97	3.16
3	−0.042	−0.088	2.29	−0.95
4	0.156	0.189	1.21	2.25
5	−0.113	0.224	3.06	2.49
6	0.025	0.086	2.27	−0.96
total			13.03	8.69

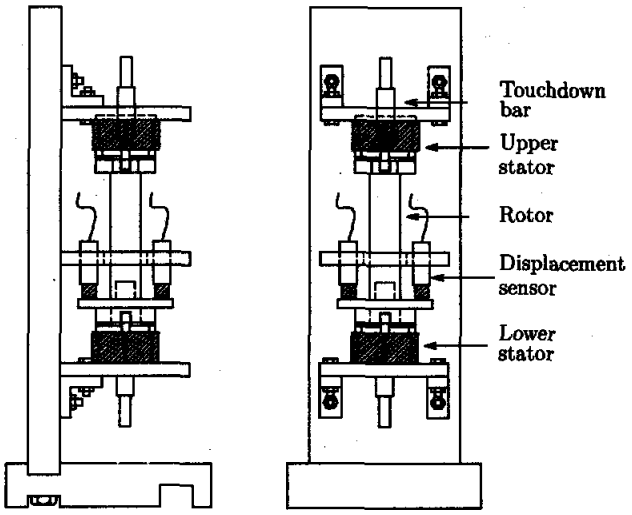

FIGURE 4: Experimental setup

used to measure the axial displacement and the tilting motions. Monitoring the tilting motions will be helpful to appraise the stability of system and to improve the design. Touch down bar, which support the rotor initially and also prevent a fatal breakdown due to the instability, which may break out, in both axial and radial direction is installed in the stator with gap $[0.3mm]$. This system is standing vertically so that the gravity cannot affect the passive stability in radial translation.

Figure 5 shows schematic diagram of a stator. In order to reduce the eddy current loss, it is made of a ferromagnetic material. The stator has six cores with coil at intervals of 60 degrees. Number of coil turns is 60. The opposite coils are connected in series, and it generates sinusoidal magnetic flux density by three phase AC currents.

Figure 6 shows schematic diagram of a rotor. The rotor consists of two yokes with four permanent magnets, a spacer, and a disk for sensor target. The yokes are made of a ferromagnetic material, while

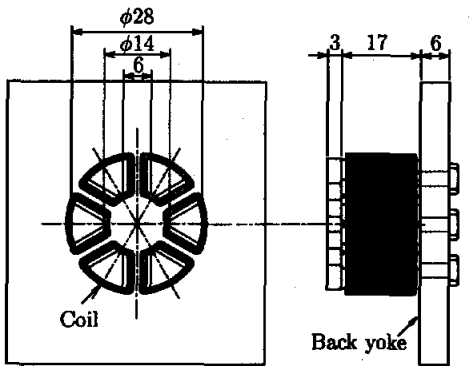

FIGURE 5: Stator

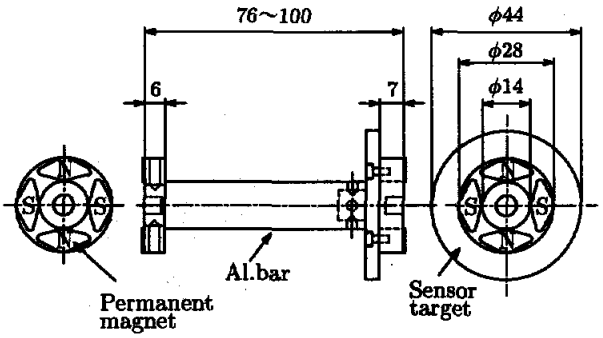

FIGURE 6: *Rotor*

the other parts including a sensor target are made of aluminum. Also, both the length of rotor and the span between stators are adjustable, which is in order to investigate the characteristics of tilting motion for various rotor lengths during the control for levitation and rotation. The length of rotor was designed to be $100mm$ and $76mm$. The weight of rotor is a maximum of about 0.1 kg at $100mm$ rotor. Moreover, the sensor target and spacer are to be removed in real system. On surfaces, the both yokes has four permanent magnets. The thickness of the permanent magnets (NEOMAX ; $Nd-Fe-B$; $\mu_r = 1.05$) is $0.7mm$.

Figure 7 shows a control system. First, the axial displacement of the rotor calculated by averaging the signals from the displacement sensors will be transformed into a digital signal processor (dSPACE DS 1103). While the synchronous speed of the rotor and the motoring currents is given by a host computer. Then, proper control signals is generated. Thereafter, through six power amplifiers, the control signals will be fed to the coils of the upper and lower stators so as to stably levitate and rotate the rotor.

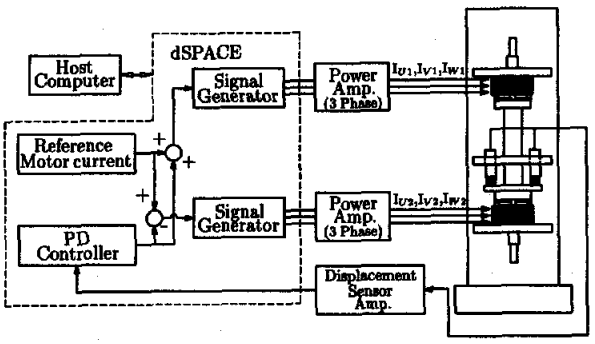

FIGURE 7: Control system

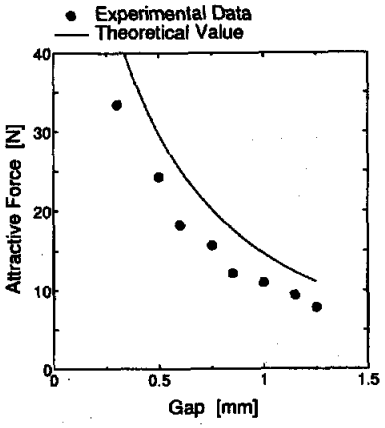

FIGURE 8: Attractive force by only PM's

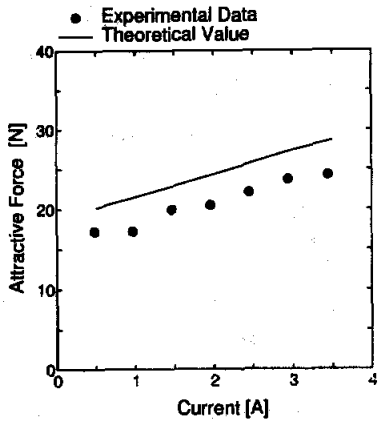

FIGURE 9: Attractive force by PM's and current when air gap is 0.8 mm

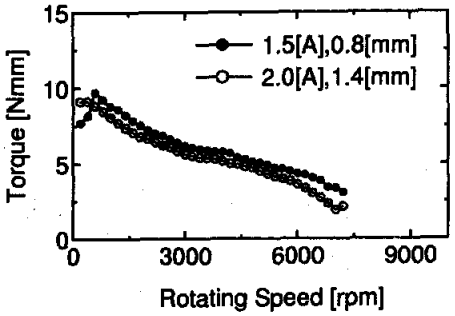

FIGURE 10: Rotating torque when $\psi = 90[deg]$

The attractive force and the motoring torque

Figure 8 shows the attractive force of the single stator generated by PM's of a rotor. We used a spring scale to measure the force. From the experimental result, the force was $12.2N$ at the nominal air gap ($0.85mm$). So, the difference between experimental data and theoretical value shown in Fig. 8 seems to come from the measurement error as well as the modeling error.

On the other hand, figure 9 shows the attractive force of the single stator generated by PM's and current of a stator at the nominal air gap. The experimental data was again measured by spring scale. From the experimental result, the force was $20N$ at the nominal state (air gap $0.85mm$, current $2A$). It is enough to support the rotor which is a maximum of about $0.1kg$. And since B_S is much smaller than B_R, the figure seems to be a linear function of current.

Figure 10 shows the motoring torque of the single stator. The experimental condition were type A (air gap $0.8mm$, current $1.5A$) and type B (air gap $1.4mm$, current $2.0A$). In the each condition, the maximum speed was $7200rpm$. Considering bidirectional type, It is enough to rotate over $10000rpm$. So, the decrease of the torque with the increase of the rotating speed seems to come from the loss at ball-bearing which is used only this experiment.

Levitated rotation

A levitated rotation experiment was conducted with the above-mentioned experimental equipment. We used a PD controller for the levitation control.

Figure 11 shows vibration amplitude of $100mm$ rotor. The control gains were selected as $K_p = 7, K_d = 0.0063, T_d = 0.3ms, \tau = 0.1ms$. The air gap was $0.85mm$ and the current was $1.5A$. From the experimental results, the axial vibration was well controlled up to 1800 rpm, while the radial vibration was relatively severe. It is naturally because of the weak stiffness in radial direction and the unbalance mass of rotor. Beyond 800 rpm, which is around the radial natural frequency, the radial motion losses its passive stability. After then, the rotor is rotating as it is in contact with the touch-down bars. The maximum speed of this proto type was near 1900 rpm, which was limited by the capacity of power amplifier. In other words, it can be due to a rotational load. As the rotational speed increases, the

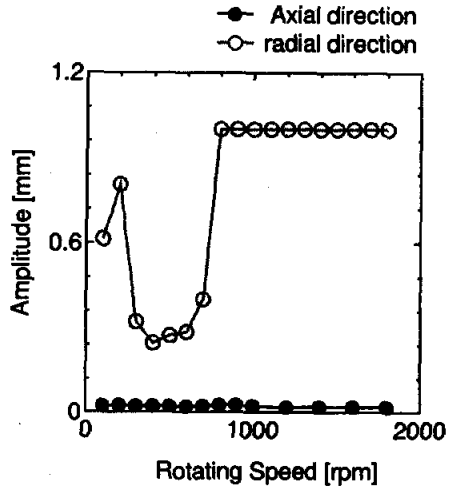

FIGURE 11: Vibration amplitude of $100mm$ rotor

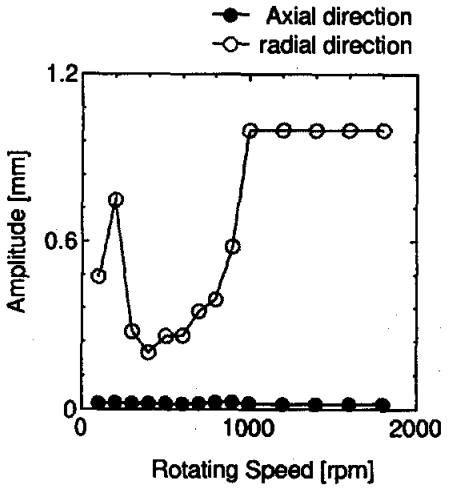

FIGURE 12: Vibration amplitude of $76mm$ rotor

phase difference between the stator and rotor fluxes becomes large and comes near 90° (electrical angle) in a synchronous motor. This means the decrease of the control force for stable levitation.

Figure 12 shows the amplitude of unbalance vibration of the 76mm rotor. Similar to the case of 100 mm rotor, the axial vibration was well controlled and the passive stability in radial motion was lost around 1000 rpm. The maximum speed was also near 1800 rpm. But by adopting a kind of lateral bearing and by increasing the capacity of power amplifier, much higher maximum speed is achievable.

Therefore, in order to stabilize the radial direction, the static pressure type air-bearing was applied in the radial direction, and it is tested again. Figure 13 shows the amplitude of unbalance vibration of the 76mm rotor with air-bearing. As a result, the motor rotates up to 10,000 rpm with stable levitation.

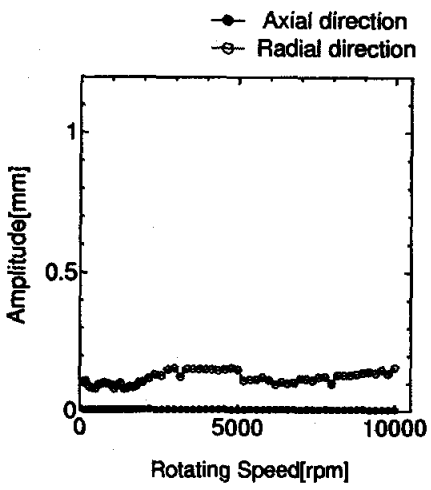

FIGURE 13: Vibration amplitude of $76mm$ rotor with air-bearing

When the motor is used in blood, it can be expected that the radial direction is stable with the fluid dynamics.

CONCLUSIONS

Aiming at a small axial pump with a levitated rotor which is leading to a small artificial heart, this paper introduces a design scheme for an axial type self-bearing motor. The experiment shows that bidirectional axial type self-bearing motor rotates near $1900rpm$. But the radial vibration was relatively severe, we could not obtain an aim of the rotating speed ($10000rpm$). Therefore, in order to stabilize the radial direction, the static pressure type air-bearing was applied in the radial direction, and it is tested again. As a result, the motor rotates up to 10,000 rpm with stable levitation. The experimental results show that bidirectional axial-type self-bearing motor has high capability for a small axial blood pump.

References

1. S Ueno and Y. Okada, Characteristics and Control of a Bidirectional Axial Gap Combined Motor-Bearing, IEEE/ASME Trans. on Mechatronics, Vol. 5, No. 3, 2000, p.310-318.

2. S Ueno et. al., Control of Axially Levitated Rotating Motor, Proceeding of the 3rd International Symposium on Motion and Vibration Control, Chiba, Japan, Vol. 1, 1996, P.94-99.